Title

Long range transmission loss of broadband seismic pulses in the Arctic under ice-free conditions

Journal

The Journal of the Acoustical Society of America, 128(4)

ISSN

0001-4966

Authors

Thode, Aaron
Kim, Katherine H
Greene, Charles R
et al.

Publication Date

2010-10-01

DOI

10.1121/1.3479686

Peer reviewed

Long range transmission loss of broadband seismic pulses in the Arctic under ice-free conditions

Aaron Thode[a)]
Marine Physical Laboratory, Scripps Institution of Oceanography, San Diego, California 92093-0205
athode@ucsd.edu

Katherine H. Kim and Charles R. Greene, Jr.
Greeneridge Sciences, Inc., 6160-C Wallace Becknell Road, Santa Barbara, California 93117
khkim@greeneridge.com, cgreene@greeneridge.com

Ethan Roth
Marine Physical Laboratory, Scripps Institution of Oceanography, San Diego, California 92093-0205
ehroth@ucsd.edu

Abstract: In 2008 the *Louis S. St-Laurent* (*LSSL*) surveyed deep Arctic waters using a three-airgun seismic source. Signals from the seismic survey were detected between 400 km and 1300 km range on a directional autonomous acoustic recorder deployed in water 53 m deep off the Alaskan North Slope. Observations of received signal levels between 10–450 Hz versus *LSSL* range roughly fit a cylindrical transmission loss model plus 0.01 dB/km attenuation in deep ice-free waters, and fit previous empirical models in ice-covered waters. The transition between ice-free and ice-covered propagation conditions shifted 200 km closer to the recorder during the survey.

PACS numbers: 43.30.Qd [AL]
Date Received: May 21, 2010 **Date Accepted:** July 19, 2010

1. Introduction

The nature of underwater acoustic propagation in the Arctic Ocean has been a subject of interest for decades, for both scientific and military reasons (Kutschale, 1961; Marsh and Mellen, 1963; Buck and Greene, 1964; DiNapoli and Mellen, 1986). An extensive body of literature exists on long-range arctic acoustic propagation, but most research has focused on acoustic propagation under deep-water ice-covered conditions, perhaps because situations where extensive ice-free conditions exist in the Arctic have been historically uncommon.

The cold surface temperatures of the Arctic yield sound speed profiles with minima at or near the ocean surface, in contrast to profiles at more temperate latitudes (Marsh and Mellen, 1963), where warmer surface temperatures at the surface result in deeper sound speed minima. Thus, in arctic conditions sound can propagate with minimal bottom interaction, potentially reducing transmission loss. However, acoustic scattering by both ice cover and surface roughness increases attenuation beyond what is typically measured for temperate deep-water propagation and what would be expected from geometric spreading losses and volume attenuation alone (Marsh and Mellen, 1963; Buck and Greene, 1964; DiNapoli and Mellen, 1986). This attenuation is strongly frequency-dependent for ice-covered waters; empirical measurements of this excess transmission loss as a function of frequency indicate an $f^{3/2}$ or f^2 relationship up to the kilohertz range, and numerous theoretical studies have sought to derive this relationship from statistical properties of ice floes and various scattering theories (Lepage and Schmidt, 1994).

[a)]Author to whom correspondence should be addressed.

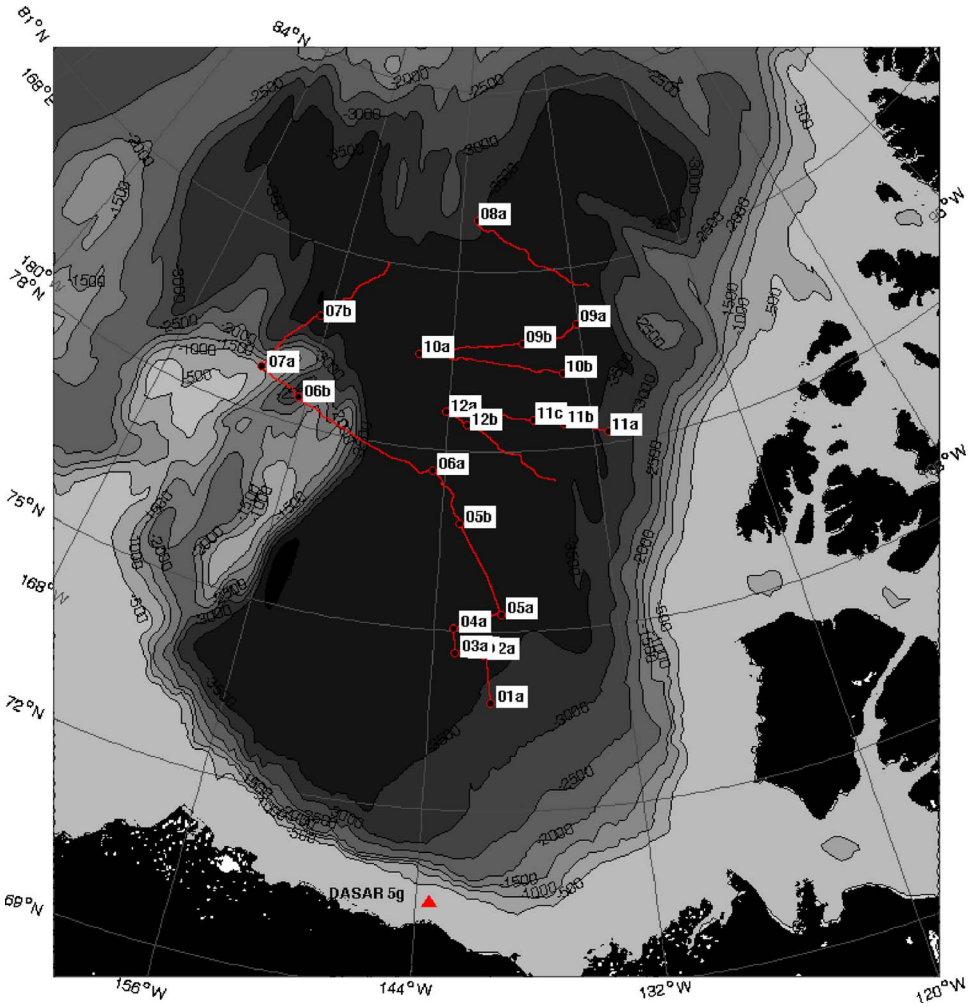

Fig. 1. (Color online) Seismic survey and acoustic receiver locations used in paper. "DASAR 5g" indicates the location of the stationary acoustic receiver. The solid lines represent the active seismic collection tracks of the *Louis S. St-Laurent* (*LSSL*) during its 2008 acquisition survey. Twelve lines of seismic profiles were acquired along a total of 21 segments (labeled a, b, and c). Black circles indicate the start/end of each line segment. The background bathymetry is shown in 500 m increments. The Northwind Ridge is the shallow bathymetric feature beneath legs 06b and 07a.

Here, we report long-range opportunistic observations of airgun pulses generated by the Canadian Coast Guard Ship (CCGS) *Louis S. St-Laurent* (*LSSL*) as part of a joint operation between the Geological Survey of Canada (GSC) and the United States Geological Survey (USGS) in 2008. Between 8/21/2008 and 10/02/2008, the icebreaker CCGS *Louis S. St-Laurent* collected 2817 km of seismic reflection profiles along 12 line segments (Jackson and Des-Roches, 2009), as summarized in Fig. 1. The *LSSL* used a cluster of three Sercel G-gun airguns as the seismic source during the survey, separated by one meter and deployed at 11.8 m depth. For the majority of the data acquisition, the total airgun volume remained constant at 1150 $in.^3$, and thus remained at constant acoustic source level. Observations of the source spectrum indicate a relatively flat output between 50 and 175 Hz, with a gentle peak in power at 72 Hz. A 8–10 dB drop-off occurs between 10 and 50 Hz and 200 and 250 Hz (Roth and Schmidt, 2010).

During this time period, a set of 35 autonomous acoustic recorders were continuously logging underwater acoustic data across a 128 km swath of the North Slope coast of Alaska. The

recorders, known as "Directional Autonomous Seafloor Acoustic Recorders" (DASARs) (Greene *et al.*, 2004), are equipped with an omnidirectional acoustic pressure sensor and two orthogonal geophones to measure the north-south and east-west components of acoustic particle velocity at frequencies between 10 and 500 Hz. The primary purpose of the deployment was to monitor the acoustic activity of bowhead whales during their fall migration westward along the North Slope coast. While recording numerous whale calls, the DASARs also recorded evidence of airgun activity from at least 4 surveys, including sounds from the *LSSL*. The following analysis uses DASAR "5g," the most seaward of the 7 DASARs at Site 5, which was located roughly north of Kaktovik at 70.4349 °N, 143.3147 °W, at a depth of 53 m (Fig. 1).

These data provide an opportunity to observe the long-range propagation characteristics of broadband signals traveling across Arctic basin-wide scales under both ice-covered and ice-free conditions, particularly since similar broadband measurements were conducted nearly 50 years ago in ice-covered waters at the roughly the same geographic location (Kutschale, 1961). While seismic airgun pulses have been detected and tracked at ranges of over 3000 km in the open Atlantic (Nieukirk *et al.*, 2004) and the Antarctic (Blackman *et al.*, 2004), this work represents the first such broadband data available from arctic waters during ice-free conditions.

2. Experimental results

2.1 Data processing

The 2008 DASAR acoustic data were processed using automated detection procedures to flag and analyze potential airgun pulses. The automated methods exploit two key characteristics of airgun pulses that differentiate them from other transient signals such as bowhead or seal sounds: a consistent regular interval between 10–20 s, and a consistent acoustic bearing, derived from the pressure and orthogonal particle velocity measurements. Thus, a series of transient detections that occurred at regular intervals and arrived within 20 degrees of a consistent azimuth were flagged as an airgun pulse sequence.

The Canadian Geological Survey provided GPS data associated with each shot conducted during the LSSL survey, from which the bearing and range of the survey relative to the DASAR could be computed. The survey bearings were then interpolated for each automated detection time of a received airgun pulse. If the interpolated bearing of the survey lay within ±20° of the flagged airgun pulse bearing, that particular airgun pulse was flagged as belonging to the LSSL.

For every LSSL airgun pulse, the root-mean-square (rms) pressure of the background ambient noise was extracted using data from the omnidirectional hydrophone, collected 1 s before the onset of the detection. The pulse sound exposure (SE) level, or time-integrated square pressure (Southall *et al.*, 2007), was then computed for the pulse. The pulse duration used for the SE was determined by measuring the time interval between the arrival of 5% and 95% of the cumulative pulse sound exposure. The rms pulse pressure is then the square root of the SE divided by the pulse duration. The sound pressure level (SPL) is 20 times the base-10 logarithm of the rms pressure. The SE level is an estimate of the energy in a pulse, while the rms pressure is a measure of the pulse's mean peak pressure. Laboratory studies indicate that the former measure may be more biologically relevant when determining the impact of an impulsive sound on marine mammal hearing (Southall *et al.*, 2007), but the latter measure has historically been more popular in the literature.

2.2 Received levels of the LSSL airgun pulses

Figure 2 depicts the broadband (10–450 Hz) *LSSL* SE levels received at DASAR 5g, as a function of the survey horizontal range *R*. Figure 2(a) shows the water depth below the *LSSL* as a function of range during times when the vessel was producing seismic sounds. The black lines indicate depth measurements made before midnight on 9/10, the date when the range of the *LSSL* from the DASAR reached its maximum value before starting to decrease again. This portion of time will be referred to as the "outgoing leg" in subsequent discussion. The circles show depths logged at times after 9/10 and will be referred to as the "returning leg." From Fig.

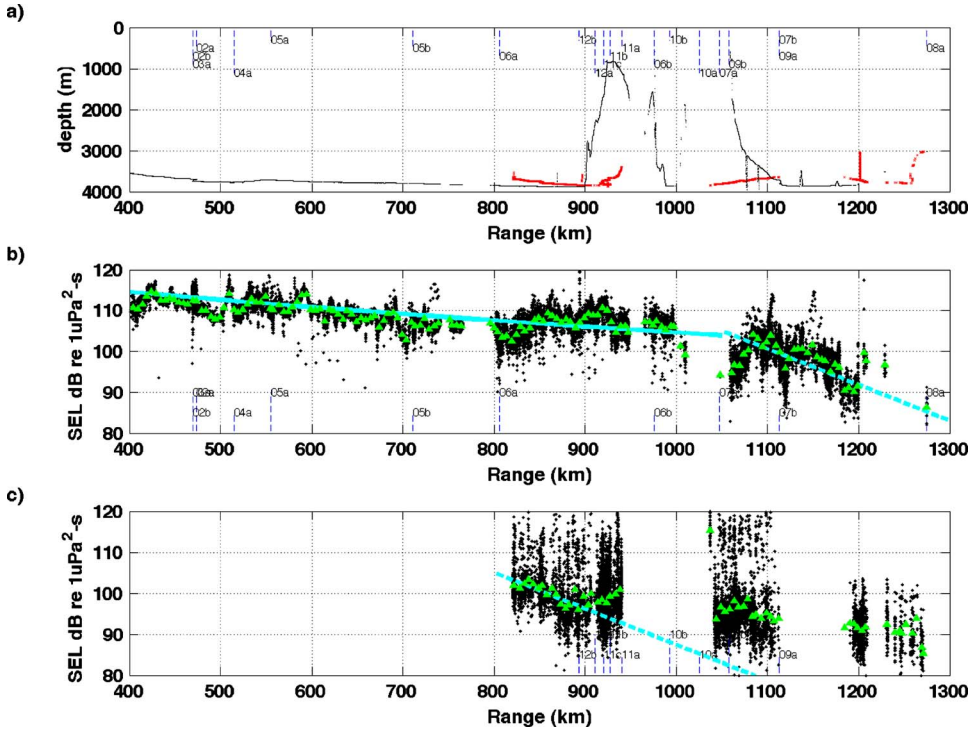

Fig. 2. (Color online) *LSSL* SE level as a function of survey range from DASAR 5g. A labeled vertical dashed line indicates the start time of each seismic segment. (a) Local water depth underneath the *LSSL* as a function of range from DASAR 5g, during times when the survey was seismically active. Thin lines indicate depth measurements made before midnight on 9/10/2008, a time period when the range between the *LSSL* and the DASAR site is monotonically increasing (the "outgoing" leg), while circles indicate times after this date, when the *LSSL* range is monotonically decreasing (the "returning" leg). (b) Received SE levels from the *LSSL* as a function of vessel range during the outgoing leg: raw values ('.') and values averaged over 5 km increments (triangles). The solid line indicates predictions of received levels from Eq. (1), assuming a 0.01 dB/km linear attenuation, while the dashed line is the prediction of received levels using the attenuation value of Eq. (2), evaluated at 72 Hz, and assuming that open water ends at 1050 km range from the DASAR. (c) Same format as above, but showing values for the returning leg. The dashed line plots Eq. (1) using the attenuation value from Eq. (2), evaluated at 72 Hz, and assuming that open water ends at 800 km range.

1 it is clear that the outgoing and return legs sample different cross-sections of the Canadian Basin, with the outgoing leg sampling the western Beaufort, and the returning leg sampling the eastern Beaufort. The dashed vertical lines indicate the starting range of each of the 12 segments of the survey shown in Fig. 1.

Figure 2(b) displays the broadband SE level for every detected pulse during the outgoing leg, using dots for the raw measurements. Range-averaged SE levels are also plotted in 5 km range increments as green triangles. The duration of most received signals is between 1 and 1.5 s, so the SPLs of the pulses are within 3 dB of the numerical SE level values. If the bandwidth of the level measurements is restricted to 250 Hz and below, the levels in Fig. 2(b) lower by about 5 dB. Figure 2(c) plots data from the returning leg, using a similar format.

Between 400 and 1110 km range the *LSSL* traversed either open water, or water covered with isolated ice floes that did not require changes in vessel course. Within hours after the start of segment 07b, the *LSSL* became surrounded by ice, and all airgun activity was conducted amidst surrounding ice cover for the remainder of the cruise.

Two simple transmission loss (TL) models overlay the measured SE level data in Fig. 2(b). The solid line between 400 and 1000 km shows the predictions of a simple cylindrical-spreading model with horizontal range R and linear attenuation α:

$$TL(dB) = 10 \log_{10} R + \alpha R. \quad (1)$$

To produce the solid line in Fig. 2, Eq. (1) has been calibrated relative to the SE level measured at 410 km range. A value of 0.01 dB/km for α produced the best fit for ice-free conditions. A simple geometric spherical spreading model produces virtually the same curve.

The two dashed lines in Figs. 2(b) and 2(c) also use Eq. (1), but with a much higher attenuation coefficient empirically derived from transmission loss curves measured during arctic winter conditions during the mid-twentieth century (Marsh and Mellen, 1963; Buck and Greene, 1964; DiNapoli and Mellen, 1986):

$$\alpha(\text{dB/km}) = 1.361\ 46 \times 10^{-4} f^{3/2}. \quad (2)$$

In Fig. 2, f in Eq. (2) has been evaluated at 72 Hz, the peak frequency of the airgun source spectrum, and the dominant frequency at ranges greater than 800 km. The two empirical transmission loss curves are calibrated to begin at 1050 km range in Fig. 2(b) and 800 km range in Fig. 2(c), for reasons presented in the discussion.

Figure 2 can be used to estimate the long-range transmission loss characteristics of the ocean between the *LSSL* and DASAR because the source level and source spectral composition of the airgun pulses remained relatively invariant with respect to time and source aspect. A review of the airgun shot schedule shows that after segment 5a, the total airgun volume fired during the cruise remained unchanged, and thus the source level remains relatively constant. Although the aspect of the seismic array relative to the DASAR changes over time, the spatial separation between airguns was only 1 m, or only 13% of a wavelength at 200 Hz, the upper frequency limit of the significant pulse energy. Thus, the source can be considered reasonably omnidirectional.

2.3 Transmission loss in ice-free waters

The *LSSL* transitioned from ice-free to ice-covered conditions between segments 7a and 7b of the survey, or between ranges of 1050 to 1100 km in Fig. 2(a). Thus, between 400 and 1000 km range, Fig. 2(b) measures propagation effects through deep ice-free conditions. Little to no published data on long-range ice-free arctic propagation conditions are available, so this portion of the survey is of particular interest. The geometric cylindrical spreading model (solid line) overlying this segment of data requires a linear attenuation factor of about 0.01 dB/km to fit the data. The bulk medium attenuation at 72 Hz is estimated to be 0.004 dB/km, or a little under half the attenuation required. The remainder might be expected to arise from surface scattering, because sound propagating from a shallow source in an arctic-style upward-refracting waveguide would interact substantially with the ocean surface. Empirical sound speed measurements from the LSSL cruise suggest a roughly linear increase of sound speed of 0.016 m/s per meter depth, yielding a circular ray path with a skip distance of 180 km (Roth and Schmidt, 2010). Thus a loss of $\sim$1 dB per surface bounce would fit the data. The corresponding Rayleigh roughness parameter Γ for this loss is 0.5, which at 72 Hz corresponds to a minimum rms surface roughness of 0.8 m, a reasonable value. Thus roughly equal contributions from bulk attenuation and surface-scattering can account for the best-fit attenuation factor. While a spherical spreading ($20 \log_{10} R$) "free space" transmission loss model also fits the observed trend, the underlying assumptions behind that model seem unrealistic for this environment.

A comparison between the survey's actual source level and received level as a function of range yields little additional insight. The actual SE source level estimated from close-range acoustic measurements was 211 dB re 1 μPa^2 s (Roth and Schmidt, 2010). If one assumes that the same propagation law in deep water holds for propagation onto the continental shelf, then a 115 dB re 1 μPa^2 s level measured at 405 km range in Fig. 2(b) yields a $17 \log_{10} R$ propagation loss factor between the DASAR and the *LSSL*, a formula that does not match either the cylindrical or spherical spreading models matched here. The fact that propagation over the continental shelf is fundamentally different than deep-water propagation most likely invalidates the assumptions used in this paragraph.

The measured transmission loss appears greater than the model at ranges between 800 and 825 km, at which point the received levels increase by 5 dB over a range of 25 km, thereby bringing the received levels in line again with the model predictions. The anomalous increase in received levels between 810 and 850 km range occurs while several events are happening simultaneously, complicating efforts to explain this increase in received level. These events include an increase in ambient noise levels around the DASAR due to storm activity, the movement of the *LSSL* into ice-covered waters, and a rapid change in bathymetric conditions as the survey approaches the Northwind Ridge.

2.4 Transmission loss in ice-covered waters

By the start of segment 7b the *LSSL* was completely surrounded by ice, which corresponds to a range of roughly 1100 km in Fig. 2. Beyond that range, the received levels on the DASAR decay much more rapidly with respect to the range of the moving source than predicted by a value of $\alpha = 0.01$ dB/km. However, the dashed line in Fig. 2(b), depicting the predicted loss for a 72 Hz signal in ice-covered waters (DiNapoli and Mellen, 1986), corresponds well with the data between 1050 and 1200 km.

While "zig-zagging" southward toward the North Slope during the returning leg, the *LSSL* received levels remained 10 dB lower than the received levels detected at the same range during the outgoing leg. During the returning leg, the vessel was continuously surrounded by ice, even to ranges of 810 km from the DASAR, because a greater extent of ice covered the entire basin at this later date, with relatively greater advances in the eastern Beaufort Sea (Department of Polar Sciences, University of Illinois at Urbana-Champaign, 2010). Thus a dashed line has been plotted in Fig. 2(c) under the assumption that ice-free conditions existed only out to 750 km range from the DASAR. The fit between the data and ice-covered propagation model for the returning leg is good between 800 and 950 km, but the received levels are higher at greater ranges. Satellite imagery provided by USGS indicates that the ice/water boundary between the DASAR and LSSL occurred between 650 and 750 km at that date (RadarSat(c), 2008).

3. Conclusion

The long-range airgun pulses generated by the *Louis S. St-Laurent* (*LSSL*) during a joint U.S.-Canadian 2008 survey in the deep-water Beaufort Sea have been automatically detected and tracked on autonomous DASAR instruments deployed on the continental shelf of the North Slope of Alaska. Airgun pulses have been detected out to nearly 1300 km range from the DASARs. The decrease in received pulse level with source range during arctic ice-free conditions is roughly consistent with a simple cylindrical spreading model, plus attenuation. The derived attenuation factor of 0.01 dB/km suggests that surface-scattering and bulk water absorption contribute roughly equal amounts of long-range attenuation in ice-free waters.

When the *LSSL* was surrounded by ice, propagation losses were much more severe with range, and the measured losses matched previous empirical estimates of propagation loss in ice-covered arctic waters. The differences between the received levels from the outgoing and return legs of the *LSSL* survey suggest that the open-water/ice boundary between the *LSSL* and the DASAR shifted toward the DASAR position by 200 km, due to advances by the regional ice field between late August and late September.

Acknowledgments

This work was supported by the U.S. Geological Survey (USGS), USGS Order No. 09-9938-3457, and conducted by Scripps Institution of Oceanography through Greeneridge Sciences, Inc. DASAR data were collected under the auspices of the Shell Exploration and Production Co. (SEPCO). Michael Macrander of SEPCO permitted access to the acoustic data. The authors are grateful for the CCGS *Louis S. St-Laurent* shot data provided by John Shimeld of the Geological Survey of Canada, Natural Resources Canada, as well as ice imagery provided by Deborah Hutchinson of the Woods Hole Science Center, USGS. The authors also appreciate the support of Jon Childs, USGS, who reviewed a draft of this work.

References and links

Blackman, D. K., Groot-Hedlin, C. C., Harben, P., Sauter, A., and Orcutt, J. A. (**2004**). "Testing low/very low frequency acoustic sources for basin-wide propagation in the Indian Ocean," J. Acoust. Soc. Am. **116**, 2057–2066.

Buck, B. M., and Greene, C. R. (**1964**). "Arctic deep-water propagation measurements," J. Acoust. Soc. Am. **36**, 1526–1533.

Department of Polar Sciences, University of Illinois at Urbana-Champaign (**2010**). "Archive of daily polar sea ice cap concentrations (1979-present)," Cryosphere Today-Historic Sea Ice Data, http://arctic.atmos.uiuc.edu/cryosphere/archive.html (Last Viewed 5/19/2010).

DiNapoli, F. R., and Mellen, R. H. (**1986**). in "Low frequency attenuation in the Arctic Ocean," in *Ocean Seismo-Acoustics*, edited by T. Akal and J. Berkson (Plenum, New York).

Greene, C. R., McLennan, M. W., Norman, R. G., Mcdonald, T. L., Jakubczak, R. S., and Richardson, W. J. (**2004**). "Directional frequency and recording (DIFAR) sensors in seafloor recorders to locate calling bowhead whales during their fall migration," J. Acoust. Soc. Am. **116**, 799–813.

Jackson, H. R., and DesRoches, K. (**2009**). "2008 Louis S. St-Laurent Field Report, August 22-October 3, 2008," Geological Survey of Canada, p. 184.

Kutschale, H. (**1961**). "Long-range sound transmission in the Arctic Ocean," J. Geophys. Res. **66**, 2189–2198.

LePage, K., and Schmidt, H. (**1994**). "Modeling of low-frequency transmission loss in the central Arctic," J. Acoust. Soc. Am. **96**, 1783–1795.

Marsh, H. W., and Mellen, R. H. (**1963**). "Underwater sound propagation in the Arctic Ocean," J. Acoust. Soc. Am. **35**, 552–563.

Nieukirk, S. L., Stafford, K. M., Mellinger, D. K., Dziak, R. P., and Fox, C. G. (**2004**). "Low-frequency whale and seismic airgun sounds recorded in the mid-Atlantic Ocean," J. Acoust. Soc. Am. **115**, 1832–1843.

RadarSat(c) (**2008**). Image Date 2008/9/26 16:28Z, as displayed on mapserver, USCG Healy 0806, courtesy of Steve Roberts, NCAR/EOL.

Roth, E. H., and Schmidt, V. (**2010**). "Noise levels generated by research icebreakers and marine seismic sources in the deep-water, Arctic Ocean," MPL Technical Memorandum No. 527, Marine Physical Laboratory, Scripps Institution of Oceanography, UCSD, San Diego, CA.

Southall, B. L., Bowles, A. E., Ellison, W. T., Finneran, J. J., Gentry, R. L., Greene, C. R., Jr., Kastak, D., Ketten, D. R., Miller, J. H., Nachtigall, P. E., Richardson, W. J., Thomas, J. A., and Tyack, P. L. (**2007**). "Marine mammal noise exposure criteria: Initial scientific recommendations," Aquat. Mamm. **33**, 411–521.